Quantifying Climate Change Hydrologic Risk at NASA Ames Research Center

GC53A-1028

William B. Mills [1], Peter D. Bromirski [2], Robert N. Coats [3], Mariza Costa-Cabral [4], Josephine Fong [5], Max Loewenstein [6], Christina Milesi [6], Norman L. Miller [5,7], Nick Murphy [8], Sujoy B. Roy [1]

[1]Tetra Tech, Inc., [2]Scripps Institution of Oceanography, [3]Hydroikos Ltd., [4]Northwest Hydraulic Consultants, [5]U.C. Berkeley, CA, [6]NASA Amers Research Center, [7]Sierra Nevada Research Institute, [8]San Jose State University, CA AUTHOR CONTACT: sujoy.roy@tetratech.com

1. Abstract

FIGURE 1: Location of the NASA Ames campus in South San Francisco Bay. The Moffett Airfield is in the foreground. Photo: NASA.

In response to the 2009 Executive Order 13514 mandating U.S. federal agencies to evaluate infrastructure vulnerabilities due to climate variability and change we provide an analysis of future climate flood risk at NASA Ames Research Center (NASA Ames) along South San Francisco Bay. This includes likelihood analysis of large-scale water vapor transport, statistical analysis of intense precipitation, high winds, sea level rise, storm surge, saturated overland flooding, and likely impacts to wetlands and habitat loss near Ames.

We use the IPCC CMIP5 data from three Atmosphere-Ocean General Circulation Models with Representative Concentration Pathways of 8.5 Wm^{-2} and 4.5 Wm^{-2} and provide an analysis of climate change associated with flooding and impacts at Ames. Intense storms impacting Ames are due to two large-scale processes, sub-tropical atmospheric rivers (AR) and north Pacific Aleutian low-pressure (AL) storm systems, both of which are analyzed here in terms of the Integrated Water Vapor (IWV) exceeding a critical threshold within a search domain and the wind vector transporting the IWV from southerly to westerly to northwesterly for ARs and northwesterly to northerly for ALs and within the Ames impact area during 1970–1999, 2040–2069, and 2070–2099. We also include a statistical model of extreme precipitation at Ames based on large-scale climatic predictors, and characterize changes using CMIP5 projections. Requirements for levee height to protect Ames are projected to continually accelerate throughout this century as sea level rises. We use empirical statistical and analytical methods to determine the likelihood, in each year from present through 2099, of water level surpassing different threshold values in SF Bay near NASA Ames.

We study the sensitivity of the water level corresponding to a 1-in-10 and 1-in-100 likelihood of exceedance to changes in the statistical distribution of storm surge height and ENSO height, in addition to increasing mean sea level. We examine the implications in the face of the CMIP5 projections. Storm intensification may result in increased flooding at Ames. We analyze how the changes in precipitation intensity will impact the storm drainage system at Ames through continuous stormwater modeling of runoff with the EPA model SWMM 5 and projected downscaled daily precipitation data.

FIGURE 2: Intense precipitation on February 3, 1998, preceded by a very wet winter, and accompanied by extreme high water levels in the South San Francisco Bay, led to flooding at NASA Ames. Photo: NASA.

Although extreme events will not adversely affect wetland habitats, adaptation projects–especially levee construction and improvement–will require filling of wetlands. Federal law mandates mitigation for fill placed in wetlands. We are currently calculating the potential mitigation burden by habitat type.

2. Wetland Mitigation Requirements for Levee Enhancements

To protect NASA Ames facilities from rising sea levels, it will be necessary to increase the elevation of flood control levees between the facilities and the Bay. Increasing the levee elevations will require placing fill material in jurisdictional wetlands, and the Corps will require in-kind mitigation, based on the footprint of the new or improved levees in the jurisdictional wetland areas.

The footprint of the levees will depend on the design elevation and the side slopes. With a side-slope of 3:1, each foot of increase in elevation will add 6 ft to the width of the footprint. The 100-yr high tide elevation (at Coyote Creek), taking account of 95 cm sea level rise and storm surge (see Figure 10 in Section 6), is estimated to be 14.8 ft NAVD88. In addition, FEMA requires at least 3 ft of freeboard on flood control levees (Schaaf & Wheeler, 2007). The preliminary design elevation of the levees is thus 17.8 ft NAVD88.

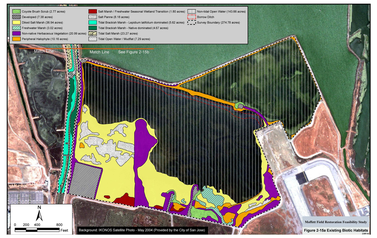

FIGURE 3: Habitat map (p.1) from H.T. Harvey & Associates, 2005.

As part of a study on the feasibility of tidal restoration in the NASA-ARC Stormwater Retention Pond (Brown and Caldwell, 2005), H.T. Harvey & Associates (HTH) mapped the "existing biotic habitats" in and adjacent to the Retention Pond (Figure 3). Alternative alignments for new levees were indicated in the report. The "no action alternative" (1b) includes a new levee along the boundary between the NASA property and the land belonging to the Mid-Peninsula Regional Open Space District. The "preferred alternative" calls for a new levee running northeast from the northeast corner of the NASA Ames Plant Engineering Yard to the levee of Pond A2E (the salt pond).

In order to measure the potential footprint of new levees we plotted the levee alignments on the HTH habitat map and measured the length of levee intersection with each habitat type. Taking account of the existing ground elevation, we calculated the width of the footprint on each side of the levee, and multiplied the width by the length of designated habitat segment. The various segments were then added to calculate the total footprint for each alternative, by habitat type. We assumed a side-slope of 8:1 (horizontal-vertical) on the outside (as recommended in the Brown & Caldwell report) and 3:1 on the inside. Table 1 summarizes the results by habitat type. The total mitigation burden if the Corps requires only 1:1 mitigation for wetland fill is thus about 20 acres for Alternative 2a and 22 acres for Alternative 1b.

Areas designated as "Herbaceous" in the table are indicated on the habitat map as "non-native herbaceous". It is not clear how much of these areas qualify as wetlands. Additional field work may be required to determine the limit of jurisdictional wetlands in these areas.

The calculations here represent the likely gross mitigation requirements for levee enhancement and construction. If the project includes removing the existing levee between Stevens Creek and the MROSD property, the restoration of the footprint of that levee could offset some of these mitigation requirements.

Due the scale of the habitat map and uncertainties in the available topographic map, these results should be considered approximate and preliminary. At the detailed design stage for levee enhancement, mitigation requirements should be measured more accurately using AutoCad or a similar spatial model.

TABLE 1. Potential Footprint of New Levees at NASA-ARC by Habitat Type

Alternative 1b	
Habitat Type	**Area, Ac**
Herbaceous	2.14
Salt Marsh / Freshwater Marsh	0.43
Diked Salt Marsh	3.95
Salt Panne	0.65
Open Water	15.04
Total Area, Ac	22.21
Alternative 2a	
Habitat Type	**Area, Ac**
Diked Salt Marsh	2.91
Salt Panne	1.69
Open Water	15.04
Total Area, Ac	19.64

3. Projected Storm Water Runoff

Storm water runoff at NASA Ames is collected in a retention pond with no outlet other than evaporation. We analyze the risk of the pond overtopping under projected rainfall extremes using bias corrected statistically downscaled daily rainfall and temperature data (Trasher et al., 2013). Predictions are for RCP 8.5 from a subset of CMIP5 models selected to represent the model genealogy as identified by Knutti et al. (2013). We model extreme runoff conditions ingesting time series of projected extreme rainfall in the hydrological model SWMM 5 (Storm Water Management Model 5).

Extreme rainfall time series are selected from each model from years with largest total winter rainfall and largest individual rainfall events.

Projections of extreme runoff are compared to historical runoff extremes (1997–1998) and to total pond depth (Figure 4). The runoff simulations suggest that under the analyzed projected extremes, large storms will become more extreme during the winter season, filling the pond earlier and closer to full capacity, with an increased risk of overtopping.

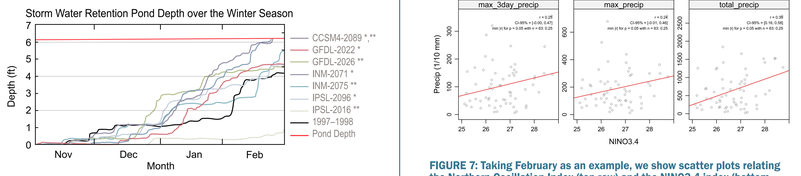

FIGURE 4: Projections of extreme runoff as modeled by SWMM 5 driven by downscaled CMIP5 projections. *Indicates simulation with time series (Nov-Feb) with extreme winter rainfall. **Indicates time series (Nov–Feb) with extreme individual rainfall event.

4. Projected Atmospheric River and Aleutian Low Storms

Projected changes in integrated water vapor transport (IVT) are analyzed for likelihoods of storm days leading to flooding at Ames. We use three IPCC CMIP5 GCMs with Representative Concentration Pathways of 8.5 Wm^{-2} and 4.5 Wm^{-2}. Intense storms impacting Ames are due to two large-scale processes, sub-tropical atmospheric rivers (AR) and Aleutian Gulf low-pressure (AL) storm systems. Both are analyzed for IVT exceeding a critical threshold within the Ames target domain with moisture advection by southerly to northwesterly wind at 850 hPa for ARs and northwesterly to northerly wind at 300 hPa for ALs for 1970–1999, 2040–2069, and 2070–2099.

APPROACH Atmospheric water vapor transport is quantified by calculating the zonal and meridional moisture transport from the surface to 300 hPa (Rasmusson 1967; Neiman et al. 2008)

$$IVT = \sqrt{\left(1/g\int_{1000}^{300}(uq)dp\right)^2 + \left(1/g\int_{1000}^{300}(vq)dp\right)^2},$$

where g is the gravitational constant (9.8 ms^{-2}), q is the specific humidity (kg kg^{-1}), and u and v are the zonal and meridional wind velocities (ms^{-1}).

We use the November to March (NDJFM) 85th percentile of the IVT histogram to determine threshold values in which flooding is likely at Ames. We impose a 5° x 5° search domain just west of Ames to determine days with integrated water vapor (IWV) greater than 2.5 cm and a steering velocity vector search for grid cells 1° just offshore to the west and 2.5° to the north and to the south of Ames, where $U=(u^2 + v^2)^{1/2}$, is at 850 hPa for ARs and 300 hPa for ALs.

Results indicate AR storm days/year at Ames for 2040–2069 with the RCP8.5 projection will increase 17–44%, for 2070–2099 RCP4.5 projected storm days/year increase 41–106%, and 2070–2099 RCP8.5 projected storm days/year increase 38–100%. Similarly, 2040–2069 RCP8.5 AL storm days/year increase 30–360%, 2070–2099 RCP4.5 increases 38–169%, and 2070–2099 RCP8.5 increases 41–317% (Table 2, Figure 5, and Figure 6). The large increase in AL days is shown to be partly due to a northward shift in the polar jet. NASA Ames is a low-lying region that will require new flood-related infrastructure protection to handle the increase in intense storms and overland flow to provide resilience from such potential increases. This suggests an evaluation of flood protection levees, and storm runoff and channel flow redirection.

TABLE 2: Changes in the Mean Number and Ratio of AR to AL Storm Days/Year for CCSM4, CM3, and ESM-LR for 1970–1999, 2040–2069 with RCP8.5, and 2070–2099 with RCP4.5 and RCP8.5. *Percent shifts in the AR to AL ratios are in parenthesis.*

Time / Model	NCAR CCSM4 AR/AL	GFDL CM3 AR/AL	MPI ESM-LR AR/AL
1970–1999	7.33/16.57 (31/69)	7.80/1.6 (83/17)	4.8/12.27 (28/72)
2040–2069, RCP8.5	8.60/27.90 (24/76)	10.0/4.67 (68/32)	7.03/15.97 (31/69)
2070–2099, RCP4.5	7.43/26.50 (22/78)	9.40/4.30 (69/31)	7.30/16.97 30/70)
2070–2099, RCP8.5	10.17/31.73 (24/76)	11.20/6.67 (63/37)	9.77/19.37 (34/66)

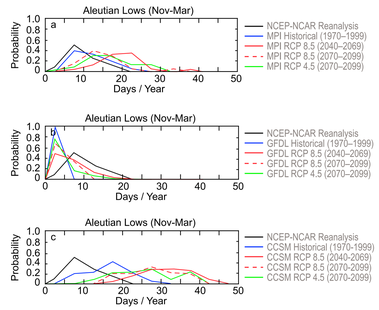

FIGURE 5: Number of AL storm days entering the Ames impact domain for a) 1970–1999, b) 2040–2069 and c) 2070–2099 with NCAR-NCEP Reanalysis (black), NCAR CCSM4 (green), GFDL CM3 (red), and MPI ESM-LR (blue) with RCP4.5 (dashed) and RCP8.5 (solid).

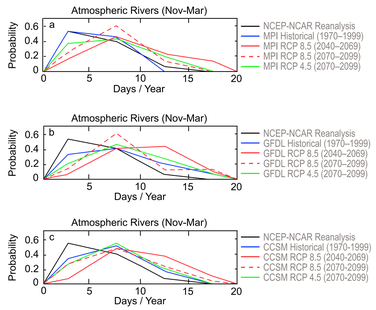

FIGURE 6: The number of AR storm days/year entering the Ames target area domain for a) MPI ESM-LR, b) GFDL CM3 and c) NCAR CCSM4.

5. Statistical Analysis of Extreme Precipitation

We are developing a statistical model of precipitation extremes at NASA Ames using climatic variables as predictors. The model will be trained for the observational period and used to project extreme precipitation in future time periods using values of the predictors variables simulated by global climate models.

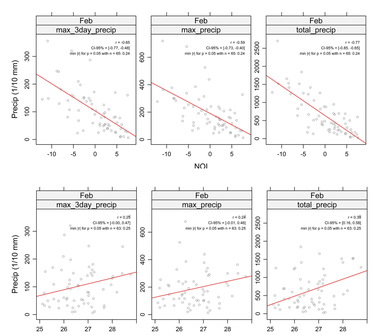

FIGURE 7: Taking February as an example, we show scatter plots relating the Northern Oscillation Index (top row) and the NINO3.4 index (bottom row) to three precipitation measures: The month's maximum 3-day precipitation total (left), maximum daily precipitation (center), and total monthly precipitation (right).

Global climate models do not yet have the ability to adequately simulate precipitation processes, and intense precipitation events in particular (e.g., DeAngelis et al. [2012], Kharin et al. [2013]). This also remains true of regional climate models, despite their finer spatial scale (e.g., Wehner, 2012, and Wehner et al., 2010). To circumvent this, statistical models of precipitation have been used in conjunction with global climate models, to produce precipitation projections (e.g., Zorita and von Storch [1999], Coles [2001], Wang and Zhang (2008), Kharin et al. [2007, 2013]). The predictors in a statistical downscaling model are larger-scale climate variables which have been shown to be strongly correlated with local precipitation, and to be adequately simulated by global climate models. The model is used under the unproven assumption (a model limitation) that in future climates this relationship will remain unchanged.

In our statistical model of extreme precipitation, we use two types of predictors. First, to predict the likelihood of storm tracks entering the San Francisco Bay area, we use two climate indices that exhibit strong correlation with local high-intensity precipitation (see Figure 7 and Figure 8): the Northern Oscillation Index (NOI) and the El Niño 3.4 Index (ENSO3.4). Second, to predict the likelihood of extreme precipitation rates, we use the specific atmospheric humidity. We train our model with the time series of daily precipitation data recorded from 1945 to present at Moffett Field (NASA Ames), and as the next step in our work (in 2014) we plan to verify and regionalize the model with daily precipitation data from several other precipitation gages in the Bay area. We started by filling the gaps in the Moffett Field data set, using recordings at the nearby San Jose and Palo Alto stations, and showing that none of several statistical tests detects in-homogeneities in the filled series.

We fit the Moffett Field daily precipitation data to an extreme value distribution, the generalized Pareto distribution (GPD), using the peaks over threshold (POT) approach (see Coles, 2001). This approach requires selection of a threshold, u, to fit exceedances to the GPD:

$$(X-u \mid X>u) \sim GPD(\sigma,\xi)$$

Where σ and ξ are linear functions of the principal components of the predictor variables (NOI, NINO3.4, and atmospheric humidity).

Threshold selection closely followed Coles (2001). We applied a cluster-identification algorithm to the precipitation time series before fitting, to remove the major effects of autocorrelation in the series. A cluster starts when precipitation on a day exceeds a specified threshold. The cluster continues until precipitation has fallen below threshold for three consecutive days. The cluster maxima are the values fit to the GPD distribution.

We fit a stationary model, i.e., where parameters σ and ξ are time-invariant, after first having used a non-stationary model (i.e., where parameters σ and ξ were linear functions of time, t) and having shown using a likelihood ratio test that there was no justification for the non-stationary model.

At the time of preparing this poster, we have not yet incorporated the specific moisture content into our model, which is our next task for the near future. Our current model uses only the two climate indices NOI and NINO3.4 as predictors. Because NOI and NINO3.4 are not independent variables, we do not use them directly but instead use their two principal components, PC1 and PC2.

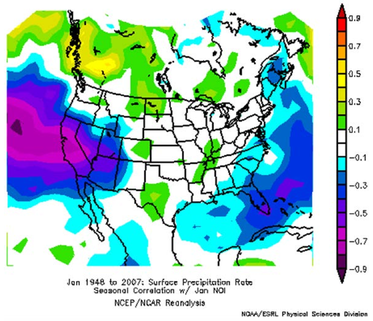

FIGURE 8: Correlation between the NOI and seasonal precipitation (December–March) in 1949–2007. NOAA's correlation web page (*www.esrl.noaa.gov/psd/data/correlation*) was used to produce this figure.

6. Statistical Analysis of Extreme Water Heights

Design of the dikes that protect the South S.F. Bay communities and property, as with most coastal defense structures in the U.S., is based on extreme water levels associated with a 100-year return period event. The understanding and characterization of the statistical behavior of high water events is based on extreme value theory, a discipline within probability theory (e.g., Coles, 2001). Despite their common basis in extreme value theory, the high-water analysis methods that are commonly employed, in the U.S. and abroad, have important differences (see Haigh et al., 2010, for a review). Methodological differences may lead to unequal levels of coastal protection, and for this reason the U.K. and Australian governments have recently defined specific methods to be applied uniformly in each of their countries (see Batstone et al. (2013) and Haigh et al (2013)). No method to estimate return periods of extreme high water events is currently applied uniformly in the U.S. Risk exposure along the U.S. Pacific and Atlantic coasts differs considerably because of the absence or near-absence of hurricanes making landfall on the Pacific coast.

To estimate the likelihood of extreme values of total water height at South San Francisco Bay locations, we use an empirical-statistical model, as described next. An hourly time series of extra-tidal water height at the San Francisco Golden Gate location (gage #9414290, record period 1901-2013) was obtained by subtracting the hourly time series of predicted tidal height (computed by NOAA on the basis of astronomic forces) fromthe detrended hourly time series of observed total water height. Because there is an observed long-term trend of increasing tidal amplitude at San Francisco (clearly noticeable in Figure 9, where the historical trend in the annual minimum is lower than the trend in the annual maximum), the detrending was performed by quantile mapping, i.e., assigning a higher trend to higher quantiles of observed water height. An extreme value distribution, the generalized Pareto distribution (GPD), was then fit to the resulting time series of extra-tidal water height using the peaks over threshold (POT) method. This methodology parallels that used for extreme daily precipitation, described elsewhere on this poster.

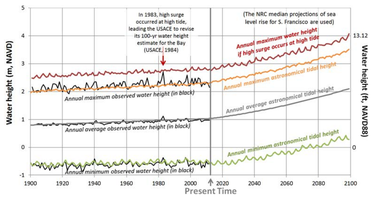

FIGURE 9: Historical and projected water height at San Francisco, Golden Gate Bridge, assuming 95 cm (3.12 ft) of sea level rise from year 2000 to 2100. The annual values plotted were derived from hourly data from NOAA for the S.F. tidal gauge (#9414290). The value used for "high surge" varies for each of the 12 months and corresponds to the 99.99th empirical percentile for that month. The red line represents total water height if this high surge were to occur in the same hour as the annual maximum water height of the astronomical tide.

Given the high degree of autocorrelation that characterizes both the tidal and extra-tidal time series,which is difficult to characterize analytically, we use an empirical-statistical method, where water levels higher than ever observed are also considered. In this method, which shares the principles underlying the USACE's empirical-statistical technique (EST), the time series of extra-tidal height is lagged in time, one hour at a time. Each time that this series is lagged, each of its values is paired with a new value of tidal height. This way, the effect of timing of joint occurrence of the tidal and extra-tidal values is taken into account in obtaining a distribution of total water height. The underlying rationale is that, when a high storm surge occurs, it could just as easily have occurred a few hours earlier or later in time, which makes the difference between it coinciding with high tide or with low tide.

Despite its length of 102 water years, the period of record is of insufficient length to adequately sample storms with a high return period. For this reason, values of extra-tidal height larger than ever observed are synthetically created by taking large observed storms and further magnifying them. These synthetic storms are then combined with the observed time series of tidal heights, to produce a distribution of total water height. The resulting probability space assigned to this synthetic distribution is the total probability assigned to these storms by the fitted GPD. The results, which are preliminary, are shown in Figure 10.

FIGURE 10: Estimated 100-year return period values of maximum water height at the San Francisco Bridge, and three South Bay locations. The white line represents the present time, and the yellow line represents the end of this century (year 2100) with a sea level rise of 95 cm (3.12 ft), corresponding to the medium estimate by NRC (2012). Results are preliminary. We use the simplifying assumption of no future changes in extra-tidal height (from ENSO effects, storm surge or wind) or hydrodynamics, which allows us to add the height of sea level rise to the white line, to obtain the projected yellow line.

References

Batstone C, Lawless M, Tawn J, Horsburgh K, Blackman D, McMillan A, Worth D, Laeger S, and Hunt T (2013) A UK best-practice approach for extreme sea-level analysis along complex topographic coastlines. Ocean Engineering 71: 28-39, DOI: 10.1016/j.oceaneng.2013.02.003.

Brown and Caldwell. 2005. Moffett Field Storm Water Retention Pond Tidal Restoration Feasibility Study. NASA Ames Research Center. Final Report.

Coles S (2001) An Introduction to Statistical Modeling of Extreme Values. Springer-Verlag, London, UK. QA273.6.C63 2001.

DeAngelis A, A Broccoli, S Decker (2012) A comparison of CMIP3 simulations of precipitation over North America with observations: Daily statistics and circulation features accompanying extreme events. J Climate. Doi: 10.1175/JCLI-D-12-00374.1.

Haigh ID, Nicholls R, and Wells N (2010) A comparison of the main methods for estimating probabilities of extreme still water levels. Coastal engineering 57: 838-849.

Haigh ID, Wijeratne EMS, MacPherson LR, Pattiaratchi CB, and George S (2013) Estimating present day extreme total water level exceedance probabilities around the coastline of Australia: tides, extra-tropical storm surges and mean sea level. Climate Dynamics. DOI: 10.1007/s00382-012-1652-1.

Kharin VV, FW Zwiers, Zhang X, Hegerl G (2007) Changes in temperature and precipitation extremes in the IPCC ensemble of global coupled model simulations. J Climate 20: 1419-1444.

Kharin VV, FW Zwiers, Zhang X, Wehner M (2013) Changes in temperature and precipitation extremes in the CMIP5 ensemble. Climatic Change, doi:10.1007/s10584-013-0705-8.

Knutti, R., D. Masson, and A. Gettelman (2013), Climate model genealogy: Generation CMIP5 and how we got there. Geophys. Res. Lett., 40, 1194–1199.

Neiman, Paul J., F. Martin Ralph, Gary A. Wick, Jessica D. Lundquist, Michael D. Dettinger, 2008: Meteorological Characteristics and Overland Precipitation Impacts of Atmospheric Rivers Affecting the West Coast of North America Based on Eight Years of SSM/I Satellite Observations. J. Hydrometeor, 9, 22–47.

Rasmusson EM (1967): Atmospheric water vapor transport and the water balance of North America: Part I. Characteristics of the water vapor flux field. Mon. Wea. Rev. 95:403-426.

Schaaf and Wheeler. 2007. Santa Clara County Drainage Manual. Santa Clara County Dept. of Planning and Developmental Services. 66 pp. plus appendices. Santa Clara, CA.

Thrasacher, B., J. Xiong, W. Wang, F. Melton, A. Michaelis and R. Nemani (2013), Downscaled Climate Projections Suitable for Resource Management, Ecs Trans. AGU, 94(37), 321.

Wang J, Zhang X (2008) Downscaling and projection of winter extreme daily precipitation over North America. J Climate 21: 923-937.

Wehner MF (2012) Very extreme seasonal precipitation in the NARCCAP ensemble: model performance and projections. Climate Dynamics. Doi: 10.1007/s00382-012-1393-1.

Wehner MF, Ri, Smith, G Bala, P Duffy (2010) The effect of horizontal resolution on simulation of very extreme United States precipitation events in a global atmosphere model. Climate Dynamics 34: 241-247. Doi: 10.1007/s00382-009-0656-y.

Zorita E, H von Storch (1999) The analog method as a simple statistical downscaling technique: Comparison with more complicated methods. J Climate 12: 2474-2489.

ACKNOWLEDGEMENT: This material is based upon work supported by NASA under award number NNX12AG33G.